Hybrid Fuzzy Logic Proportional Plus Conventional Integral-Derivative Controller for Permanent Magnet Brushless DC Motor

Bhim Singh, A.H.N.Reddy, S.S.Murthy
Department of Electrical Engineering,
Indian Institute of Technology, Delhi, India-110016
bsingh@ee.iitd.ernet.in

ABSTRACT: This paper presents a hybrid fuzzy logic proportional plus conventional integral-derivative controller (FP+ID) for the speed control of permanent magnet brushless dc (PMBLDC) motor. Though, PID controllers are commonly used in practice, they have failed to perform satisfactory under nonlinearity, load disturbances, parameter variation etc. In this paper, the performance of the permanent magnet brushless dc motor drive is examined with a hybrid controller which is a combination of fuzzy logic and conventional controller. This controller shows improved performance compared to PID speed controller.

I INTRODUCTION

Permanent magnet brushless motors have found wide applications due to their high power density and ease of control. Moreover the brushless dc motor has high efficiency, low maintenance and low rotor inertia that have increased the demand of brushless DC motors in high power servo and robotic applications [11. The invention of modem solid state devices like MOSFET, IGBT, MCTs and high energy rare earth PMs have widely enhanced the applications of PMBLDC motors in variable speed drives. The modeling, detailed simulation and experimental verification of this drive has been discussed in [2-51.

There has been tremendous research for providing suitable speed controller for PMBLDC motor. Many control strategies have been proposed till today. The main drawback of fixed gain controllers is that their performance deteriorates as a result of changes in system operating conditions. This has resulted in the increased demand of modem nonlinear control structures. Very few adaptive controllers have been practically employed in the control of electric drives due to their complexity and inferior performance [6].

, Fuzzy logic though developed many years ago, has recently emerged as a useful tool in industrial control applications. It is well known that this control technique depends on human capability to understand system's behavior and also on control rules. Fuzzy controllers have been successfully used for many years 17-121. These controllers are inherently robust to load disturbances. Another advantage **is that** fuzzy logic controllers can be easily be implemented. The combination of intelligent control with robust control appears today the most promising research accomplishment in the area of drive control.

The applications of fuzzy controllers are limited because of some drawbacks. **In** order **to eliminate them,** many researchers are now combining fizzy logic and conventional techniques. Li[13] has presented an approach to the design **of** a **hybrid** fuzzy **proportional plus conventional integral-derivative controller. According to him, one of the purposes** for **proposing the fuzzy P+ID controller is to improve control performance of many industrial plants that are already controlled by PID controllers.**

In this paper, we explore the feasibility of hybrid FP+ID controller for the speed control of PMBLDC motor drive. In this, the proportional term in the conventional PID controller is replaced with an incremental fuzzy logic controller improving the behavior of conventional PID controllers. This controller uses hzzy rules that are based on eliminating the overshoots. Our results show significant improvement in both transient and steady state responses of the drive. Unlike PID controller, this controller makes the PMBLDC drive more robust to load variations. The key feature of this scheme is to compensate for overshoots **and oscillations in the response of the PMBLDC motor.**

This **paper** is organized as **follows. In section 11, the basic components of PMBLDC motor drive is described. Different** components **of** the **drive** system **like speed controller, current controller and inverter are analyzed in section 111. The present scheme is simulated under real time operating conditions and compared with PID controller in section IV. Finally main** observations are concluded **in** section V.

I1 DESCRIPTION OF THE DRIVE SYSTEM

Fig1 describes the basic building blocks of the PMBLDC motor drive. The drive consists of proposed FP+ID Controller, reference current **generator,** PWM **current controller, position sensor, motor and MOSFET based** inverter. The speed of the motor is **compared with its reference value and the error in speed is processed in FP+ID** controller. The **output** of this controller is **considered as the reference torque. A limit is put on the speed controller output** depending on maximum winding **currents. The reference current generator block generates the three phase reference currents (i_a*, i_b*, i_c*) using the limited peak current magnitude decided by the controller and the position sensor. The reference currents have the shape of quasi-square wave in phase with respective backemfs to develop constant unidirectional torque. The PWM current controller regultes the winding currents (i_a, ib, i_c) with in the small band around the reference currents (i_a*, ib*, &*). The motor currents are compared with the reference currents and the switching commands are generated to drive the inverter devices.**

I11 ANALYSIS OF PMBLDC DRIVE

The drive system considered here consists of FP+ID controller, the reference current generator, PW current

controller, PMBLDC motor and MOSFET inverter. All these components are modeled and integrated for simulation in real time conditions.

3.1 **FP+ID** controller structure

Fig.1 illustrates the basic control structure of FP+ID speed controller. This hybrid fuzzy controller has the advantages of PID controller along with fuzzy. The control signal of conventional PID speed controller described below.

$$\omega_{e(n)} = \omega_{r(n)}^{*} - \omega_{r(n)}$$
$$\Delta\omega_{e(n)} = \omega_{e(n)} - \omega_{e(n-1)}$$
$$T^{*}_{(n)} = T^{*}_{(n-1)} + K_P\{\omega_{e(n)} - \omega_{e(n-1)}\} + K_I + K_D\{\omega_{e(n)} - 2\omega_{e(n-1)} + \omega_{e(n-2)}\} \quad (1)$$

where K_p, KI and K_D are the controller gains of PID speed controller. n is a sampling index.

The control signal of the present scheme is given by

$$T^{*}_{(n)} = T^{*}_{(n-1)} + K_P \times \Delta\hat{u}(k) + K_I\, \omega_{e(n)} + K_D\{\omega_{e(n)} - 2\omega_{e(n-1)} + \omega_{e(n-2)}\} \quad \textbf{(2)}$$

where Kp, K_I and K_D are identical to the fmed gain PID speed controller, $\Delta\hat{u}(k)$ is the output of the fuzzy logic controller. The output of the above equation T^* is considered as the reference torque of the PMBLDC motor. The dominating term in FP+ID controller is the proportional gain, which is responsible to reduce overshoot and rise time.

$$\Delta\hat{u}(k) = FLC[\omega_{e(n)}, \Delta\omega_{e(n)}] \quad (3)$$

where $\omega_{e(n)}$ is the error between reference speed and speed of the motor and $\Delta\omega_{e(n)}$ is the change in speed error.

Now we describe the fuzzy logic term $\Delta\hat{u}(k)$ = FLC[$\omega_{e(n)}$, $\Delta\omega_{e(n)}$]. $\omega_{e(n)}$,and $\Delta\omega_{e(n)}$ are the inputs to the fuzzy logic controller and $\Delta\hat{u}(k)$ is the output. The fuzzy members are chosen are as follows:

positive big: PB	negative big: NB
positive medium: PM	negative medium: NM
positive small: PS	negative small: NS
and zero: ZO	

Moreover, the triangular-shaped functions are chosen as the membership functions due to the resulting best control performance and simplicity. The height of the membership functions in this case is one, which occurs at the points -1, -0.57, -0.27, 0, 0.27, 0.57,1 respectively as shown in Fig.Z(a). 50% of overlap has been provided for neighboring fuzzy subsets. Therefore, at any point of the universe of discourse, no more than two fuzzy subsets will have nonzero degrees of membership. The realization of the function FLC[$\omega_{e(n)}$, $\Delta\omega_{e(n)}$], based on the standard fuzzy method, consists of three stages: fuzzification, Inference method, and defuzzification.

Fuzzifcation: This converts point-wise (crisp) data into fuzzy sets (linguistic variable), making it compatible with fuzzy representation.

Znfererrce method A linguistic rule table, according to the dynamic performance of the drive is shown in Table l. The first two linguistic values are associated with the input variables $\omega_{e(n)}$ and $\Delta\omega_{e(n)}$ while the third linguistic value is associated with the output. For example, if error in speed is ZO and change in speed error is NS, then output is NM.

Defuzzijication: The reverse of fuzzification is called defuzzification. The rules of FLC produce required output in a linguistic variable. Linguistic variables have to be transformed to crisp output. By using the center of gravity (COG) defuzzification method, crisp output is obtained.

3.2 Reference current generator

The magnitude of the three phase current (I^*) is determined by using reference torque (TO) and the back emf constant (K_b) as: $I^* = T^*/K_b$. Depending on the rotor position, the reference current generator generates the reference currents (i_a^*, i_b^*, i_c^*) by taking the value of reference current magnitude as I^*, $-I^*$ and zero.

Rotor Position Signal	Referznce Currents
	U 1: ic
0"-60"	f -f 0
60"-120"	I* 0 -I'
120"-180"	0 I* -I'
180"-240"	-I0 f 0
240"-300"	-I' 0 I^b
300"-360"	0 -I' I*

These reference currents are fed to the PWM current controller.

3.3 PWM Current Controller

The switching logic is formulated as given below.

If $i_a < (i_a^* - h_b)$ switch 1 ON and switch 4 OFF
If $i_a > (i_a^* + h_b)$ switch 1 OFF and switch 4 ON
If $i_b < (i_b^* - h_b)$ switch 3 ON and switch 6 OFF
If $i_b > (i_b^* + h_b)$ switch 3 OFF and switch 6 ON
If $i_c < (i_c^* - h_b)$ switch 5 ON and switch 2 OFF
If $i_c > (i_c^* + h_b)$ switch 5 OFF and switch 2 ON

Where h_b is the hysteresis band around the three phase reference currents.

3.4 Modeling of back emf using rotor position

The per phase back emf in the PMBLDC motor is trapezoidal in nature and are the functions of the speed and rotor position angle (θ_r). The normalized function of back emfs is shown in Fig.2(c). Froni this, the phase back emf e_{an}, can be expressed as:

$e_{an} = E$ $0° < \theta_r < 120°$
$e_{an} = (6E/\pi)(\pi - \theta_r) - E$ $120° < \theta_r < 180°$
$e_{an} = -E$ $180° < \theta_r < 300°$
$e_{an} = (6E/\pi)(\theta_r - 2\pi) + E$ $300° < \theta_r < 360°$

where $E = K_b\, \omega_r$ and e_{an} can be described by E and normalized back emf function $f_a(\theta_r)$ shown in Fig.Z(c). $e_{an} = E\, f_a(\theta_r)$. The back emf function of other two phases e_{bn} and e_{cn}, are defined in similar way using E and the normalized back emf function $f_b(\theta_r)$ and $f_c(\theta_r)$ as shown in Fig.Z(c).

3.5 Modeling of PMBLDC Motor and Inverter

The PMBLDC motor is modeled in the 3-phase abc variables. The general volt -ampere equation for the circuit shown in the Fig.2(b) can be expressed as:

$$v_{an} = Ri_a + p\lambda_a + e_{an} \quad (4)$$
$$v_{bn} = Ri_b + p\lambda_b + e_{bn} \quad (5)$$

V_{cn}=Ri,+ph,+e, (6)

where v_{arlr} V_b) and v,, are phase voltages and may be designed as:

van = V_{ao}- VI,,, V_{bn}= V_{bo} - V,, and V,, = V,, - V,,. (7)

Where v,,, V_{bor} v, and v,, are three phase and neutral voltages referred to the zero reference potential at the mid-point of dc link (0) shown in the Fig.S(b). R is the resistance per phase of the stator winding, p is the time differential operator and e,,,,, e_b, and e,, are phase to neutral back emfs.

The h_a, h_b and *h*, are total flux linkage of phase windings a, b and c respectively. These values can be expressed as:

^ = L,i, - M(i_b + i,) (8)

h_b=L,i_b-M(i_a + i,) (9)

^ = L,i,-M(i,+i_b) (10)

Where L, and M are the self and mutual inductance, respectively.

The PMBLDC motor has no neutral connection and hence this result in:

i_a+i_b+i,=O (11)

Substituting equation (11) into equations (8), (9) and (10) the flux linkages are given as:

L_a= i_a(L_s + M), h_b= &(L_a + M)mdh,= i,& + M) (12)

By substituting equation (12) in volt-ampere equations (4) - (6) and rearranging these equations in a current derivative of state space form, one gets

pi, = l/(L,+M) (v_{an} - Ri_a - ej (13)

pi_b=l/(L,+M)(v_b-Ri_b-e_b,) (14)

pi,=l/(L,+M)(v,,-Ri,-e,,) (15)

The Developed electromagnetic torque may be expressed as:

T, = (e_{an} i, + e_{bn} i_b+ e,, i,) / a, (16)

where o_r is the rotor speed in electrical radsec.

The mechanical equation of motion in speed derivative form can be expressed as:

PO, = (P/2) (T, - TI. B 0,) /J (17)

where P is the number of poles, TI is the load torque in N-m, B is the frictional coefficient in N-ms/rad, and J is the moment of inertia, kg-m^2.

The derivative of the rotor position (0,) in state space form is expressed as:

pe_r=O_r (18)

The potential of the neutral point with respect to the zero potential (v,,) is required to be considered in order to avoid inbalance in the applied voltage and simulate the performance of the drive.

This can be obtained as follows:

Substituting equation (11) in the volt-ampere equations (4) to (6) and adding them together gives:

v,, +v_{bo} +v_{c0} - 3v,, = R(i,+ i_b+ i,) + (L, + M) (pi_a+ pi_b + pi,) + (e_m4-e_{bn}'e_{cn}) (19)

Substituting equation (11) in equation (19) we get:

v_{ao}+v_{bo} +V_{CO} - 3V_{no} = (e_m + e_{bn}+e_{cn})

Thus, v,,,, = {V_{ao} +V_{bo} +V_{co} - (e_{an} + e_{bn}+e_{cn})) 1 3

The set of differential equations mentioned in eqns (13), (14), (15), (17) and ('*) defines the developed mode' in terms Of the variables i,, i_b, i,, o_r, 0, and time as an independe-nt variable.

IV RESULTS AND DISCUSSIONS

An algorithm is developed to simulate the drive model with both the FP+ID speed controller and fixed gain PID controller. The set of equations representing the model of the drive system is discussed in previous section. Runge-Kutta numerical integration method is used to get the solution of these equations. The transient and steady state responses of a 3 phase, 2.0h.p, 4 pole, 1500rpm, 4A PMBLDC motor are shown in Figs. 3 to 6. It is to evaluate the performance of the FP+ID controller for the speed control of PMBLDC motor during different operating conditions. The PID gain parameters used for our real time simulation are listed in APPENDIX-I. The same values of PID control gains are used for both FP+ID speed controller and conventional PID controller to examine the performance of drive with these two controllers. The specifications of the PMBLDC motor are given in APPENDIX-11.

4.1 Starting response of the PMBLDC drive

Fig.3 shows the rotor speed, winding current, developed torque of the PMBLDC drive from standstill to a speed of 157radsec (1500rpm). It is observed that the drive takes 180msec to reach the set speed. The FP+ID speed controller comes in to action and tracks the reference speed of 1500rpm. It is clear from Fig.3 that the speed response has no overshoots and oscillations. The starting response of the PMBLDe drive with PID controller is shown in Fig.4. The response of the drive is slower than that of FP+ID speed controller. This controller shows an overshoot in speed response, which is undesirable. The drive takes maximum permissible current to start the motor from standstill. It is observed from the results that the response of the drive is faster with FP+ID controller than the conventional controller and shows improved response compared to PID controller.

4.2 Performance of the drive under speed reversal

The motor running under steady state with a speed o! 157radsec which is suddenly changed to other direction at tz1.Osec. The controller makes the motor speed to coincide with the reference speed. Fig.3 shows the speed response of the drive with FP+ID controller under speed reversal. The drive takes 290msec to reach the set speed of -157raUsec. The response is smooth and no oscillation in the case of present control scheme. This is due to robust and accurate control of the structure of the present controller. The speed reversal response of the drive with PID controller is shown in Fig.4. The drive takes 350msec for speed reversal. The results show superior results of the FP+ID controller over PID controller.

4.3 Performance of the drive under load change

Fig.5 shows the performance of the FP+ID speed controller under load perturbation. The sudden application of load at tz0.7 and removal at t= l.l.sec on the motor shaft cause a negligible change in the speed response of the drive. The FP+ID controller makes the drive robfist to load variations. The torque rises to 3Nm and remains at the same value till the load is removed. The response of the drive under load perturbation (applying load at t=O.llsec and removal at t= l.l sec) with fixed gain PID controller is shown in Fig.6. The dip in speed is around 5radsec (47.75rpm) with the conventional PID controller as shown. The drive takes lOOmsec for recover to the original speed. Under sudden removal of load, the rise in speed is 4 rads. The results show significant improvement in the response of the drive with the FP+ID speed controller

V CONCLUSIONS

A hybrid controller (FP+ID) controller has been employed for the speed control of PMBLDC motor drive. A performance comparison between the present controller and conventional PID controller has been carried out by several simulation confirming the superiority of the FP+ID controller. The results have shown that this speed controller is robust to external load disturbances. For implementing the FP+ID controller, only an additional parameter has to be adjusted such that manual tuning time of the controller can be significantly reduced. The performance of the PMBLDCM drive, both in steady state and dynamic conditions, is found to be good with FP+ID speed controller.

REFERENCES

[1] T.J.E.Miller, "Brushless Permanent magnet and Reluctance Motor Drives", Oxford Science Publication, 1993.

[2] P.Pillay and R.Krishnan, "Modeling, simulation and analysis of a Permanent magnet brushless DC motor drive", IEEEDAS Meeting, 1987, pp. 8-14.

[3] T.Sebastian and G.R.Slemon, "Transient Modeling and Performance of Variable Speed Permanent Magnet Motors", IEEE Trans. on IA, Vo1.25, No.1, JadFeb 1989, pp. 101-106.

[4] A.Rubai and R.C.Yalamanchi, " Dynamic study of an electronically brushless DC machine via computer simulations", IEEE Trans. on EC, Vo1.7, No. 1, March 1992, pp. 132-137.

[5] P.C.K.Luk, C.K.Lee, "Efficient modeling for a brushless DC motor drive", IEEEAECON, 1994, pp.188-191.

[6] E.Cenuto, A.Consoli, A.Raciti and A.Testa, "A robust adaptive controller for PM motor drives in robotic application", IEEE Trans. on PE, Vol. 10, No.1, Jan 1995,pp.62-71.

[7] C.C.Lee," Fuzzy logic in control systems: Fuzzy logic conkol —part1 & part2", IEEE Trans. Syst., Man, Cybernetics., V01.20, No.2, MarlApr.1990, pp. 404-435.

[8] G.C.D. Souza and B.K.Bose ,"A Fuzzy Set Theory based control of a Phase-Controlled Converter DC Machine Drive", IEEE Trans. on IA, V01.30, No.1, Jan/Feb 1994, pp. 34-44.

[9] S.A.Mir, DSZinger and M.E.Elbuluk, "FUZZY controller for inverter fed induction machines", IEEE Trans. on IA, Vo1.30, No.1, JanlFeb 1994, pp. 78-84.

[10] C.S.Indulkar and B.Raj, "Application of Fuzzy controller to Automatic Generation Control, Journal of Electrical Machines and Power Systems, Vol. 23, No.2, MarIApr 1995, pp. 209-220.

hthe P.Mattavelli, L.Rossetto, GSpiazzi, P.Tenti, "General purpose Fuzzy controller for DC-DC Converters", IEEE Trans. on PE, Vol.12, No.I, Jan 1997, pp.79-86.

[12] E.Cenuto, A.Consoli, A.Raciti and A.Testa, "Fuzzy. Adaptive Vector Control of Induction Motor Drives", IEEE Trans. on PE, Vol. 12, No.6, Nov 1997, pp. 1026-1040.

[13] W.Li, "Design of a Hybrid Fuzzy Logic Proportional Plus Conventional Integral-Derivative Controller", IEEE Trans. on Fuzzy Systems, Vo1.6, No.4, Nov 1998,pp.449-463.

[14] J.S.Ko, "Robust position control of BLDC motors using Integral-Proportional-Plus Fuzzy logic controller", IEEE Trans. on IE, Vo1.41, June 1994, pp.308-315.

APPENDIX-I

The controller gains of both the controllers are same and given here:

K_p=O.l, K,=0.0005 and K_D=0.0012.

APPENDIX-I1

Rating	: 2.0 h.p
No. of Poles	:4
Type of connection	: Star
Rated Speed	: 1500rpm
Rated current	:4A
ResistanceIPh	:2.8R
Back EMF Constant	: 1.23VSeclrad
Self & Mutual Inductance	: 0.00521 H/phase
Moment of Inertia	: 0.013 Kg-m'

TABLE 1 Fuzzy logic rules for FP+ID speed controller

e\ce	NB	NM	NS	ZO	PS	PM	PL
NB	NB	NB	NB	NB	NM	NS	ZO
NM	NB	NB	NB	NM	NM	ZO	PS
NS	NB	NB	NM	NS	ZO	NS	PM
ZO	NB	NM	NS	ZO	NS	PM	PB
PS	NM	NS	ZO	PS	PS	PS	PS
PM	NS	ZO	I'S	Ph	PB	PB	PB
PB	ZO	PS	PM	PB	PB	PB	PB

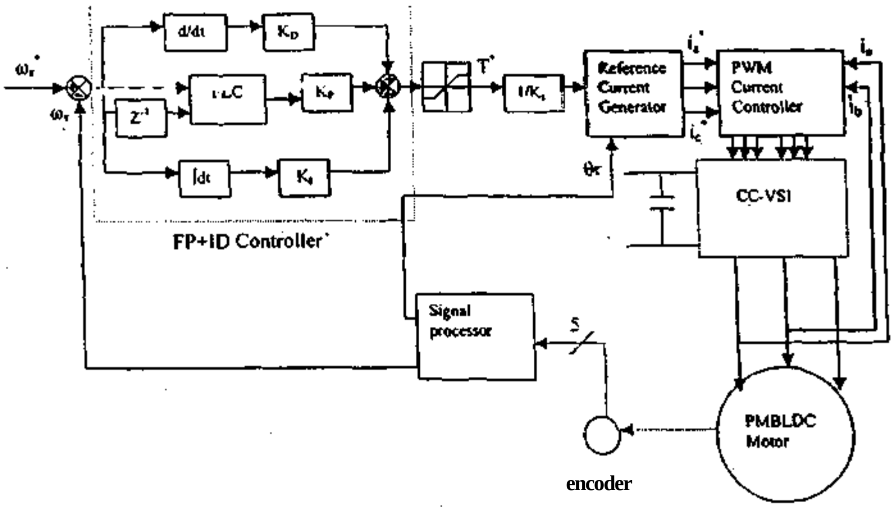

Fig.1 Basic block diagram of PMBLDC rootor drive system

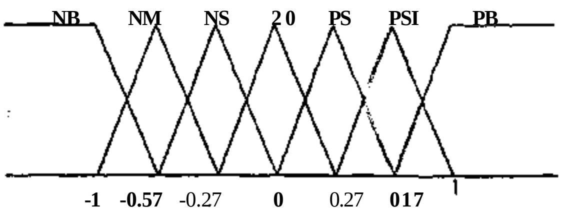

Fig.2(a) Membership f u n c t b

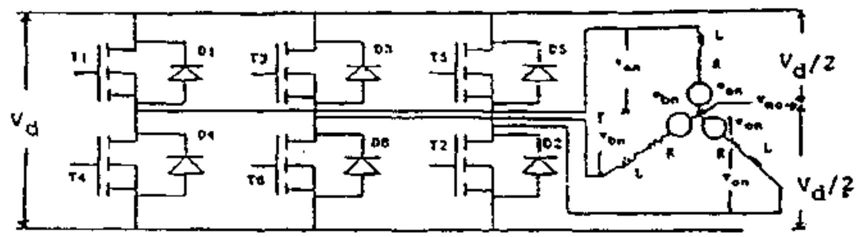

Fig.Z(b) Inverter circuit with **P\lBLDC** drive

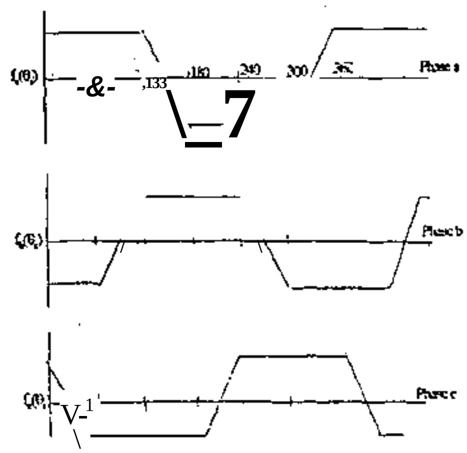

Fig.2(c) Furictions of back crnfs of PYELDC riiotor

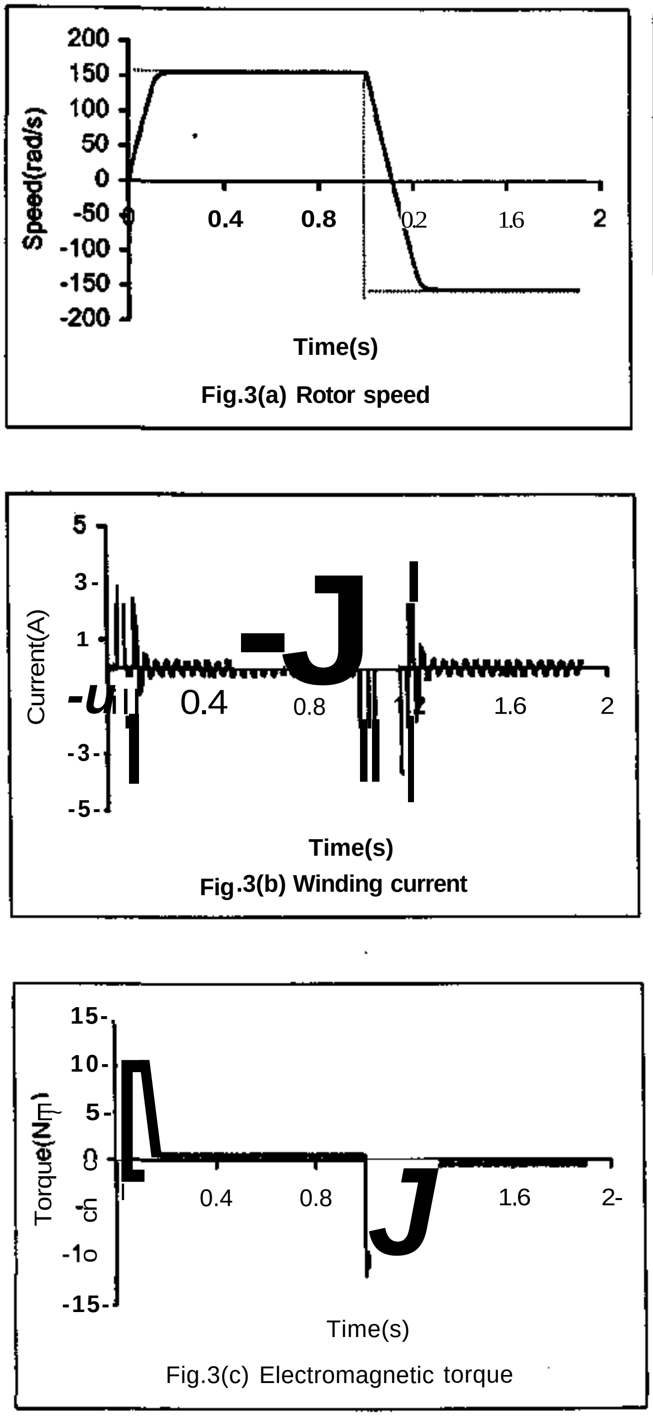

Fig.3(a) Rotor speed

Fig.3(b) Winding current

Fig.3(c) Electromagnetic torque

Fig.3 Performance of the PMBLDC drive with FP+ID controller during starting and speed reversal.

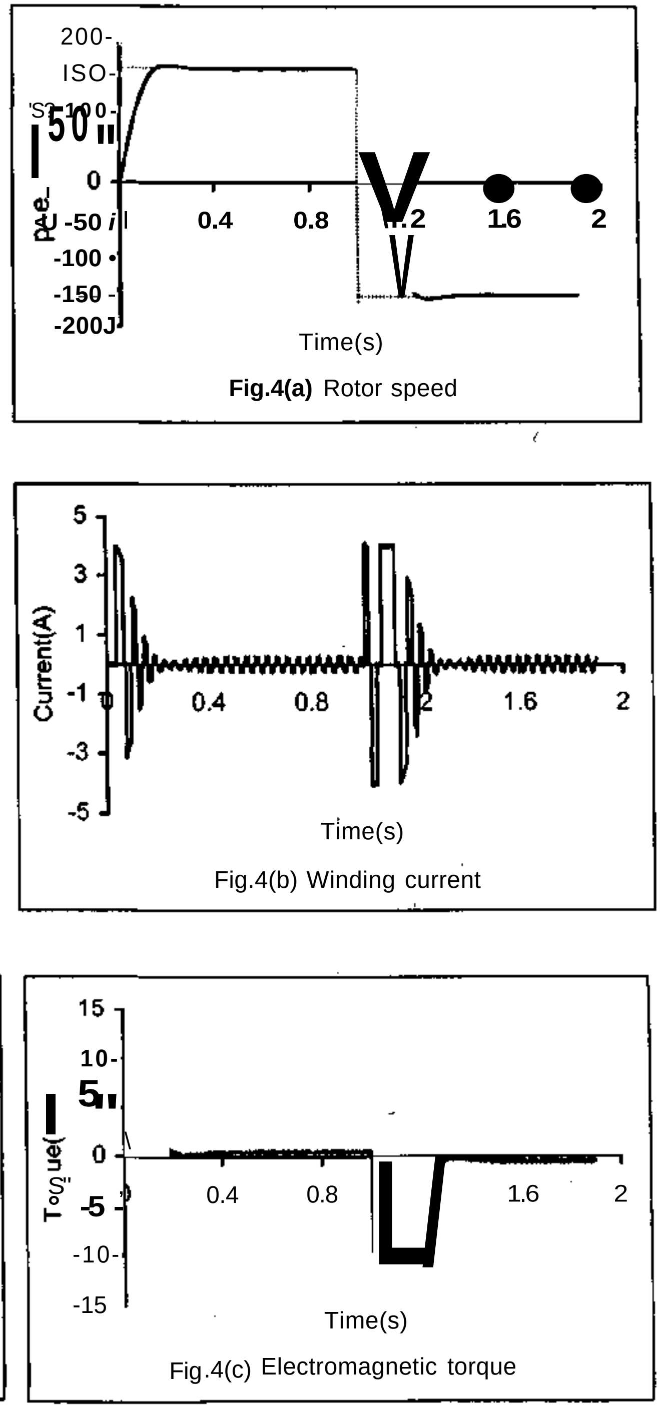

Fig.4(a) Rotor speed

Fig.4(b) Winding current

Fig.4(c) Electromagnetic torque

Fig..? Performance of the PMBLDC drive with PID controller during starting and speed reversal.

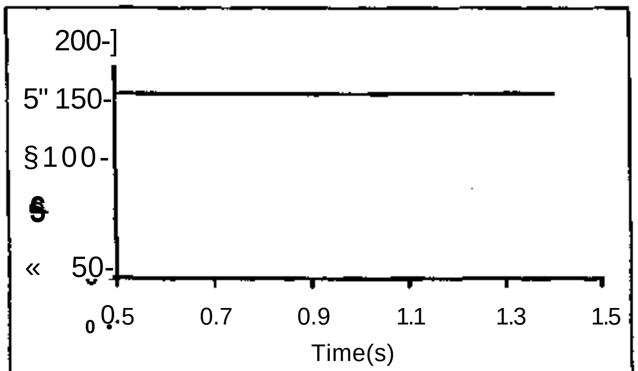

Fig.S(a) Rotor speed

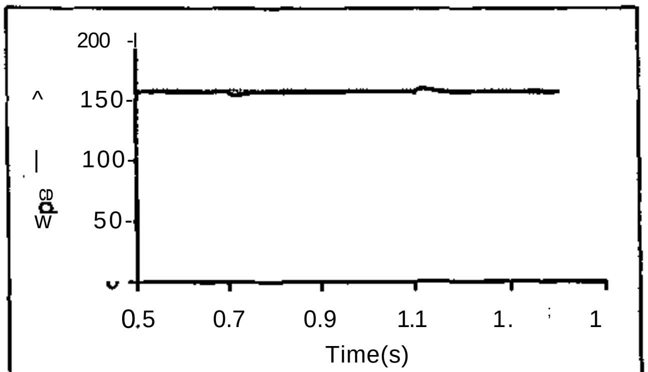

Fig.G(a) Rotor speed

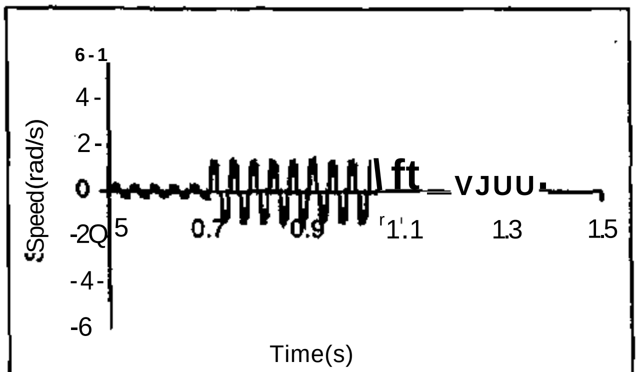

Fig.S(b) Winding current

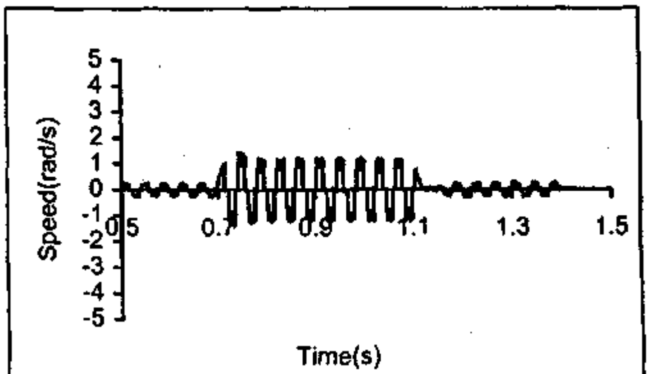

Fig.G(b) Winding current

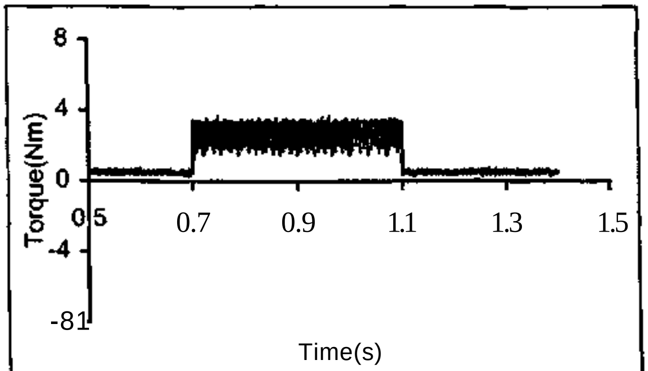

Figs(c) Electromagnetic torque

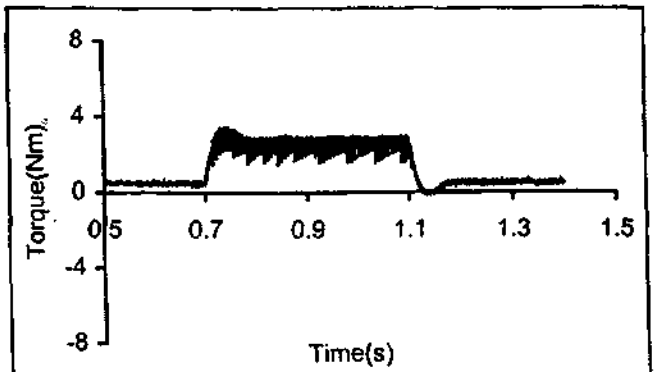

Fig.6(c) Electromagnetic torque

Fig.5 Response of the PMBLDC motor with the FP+ID speed controller during load perturbation

Fig.6 Response of the PMBLDC motor with the conventional PID controller **during load** perturbation